Surface Defects and Bulk Defect Migration Produced by Ion Bombardment of Si(001)

K. Kyuno, David G. Cahill, and R. S. Averback
Department of Materials Science and Materials Research Laboratory, University of Illinois, Urbana, Illinois 61801

J. Tarus and K. Nordlund
Accelerator Laboratory, University of Helsinki, P.O. Box 43, FIN-00014, Finland

(Received 14 June 1999)

Variable-temperature scanning tunneling microscopy is used to characterize surface defects created by 4.5 keV He ion bombardment of Si(001) at 80–294 K; surface defects are created directly by ion bombardment and by diffusion of bulk defects to the surface. The heights and areal densities of adatoms, dimers, and adatom clusters at 80 and 130 K are approximately independent of temperature and in reasonable agreement with molecular dynamics calculations of adatom production. At 180 K, the areal density of these surface features is enhanced by a factor of ~ 3. This experimental result is explained by the migration and surface trapping of bulk interstitials formed within ~ 2 nm of the surface.

PACS numbers: 61.80.–x, 61.72.Ji, 68.35.Dv

The properties of point defects, and their interactions with impurity atoms and extended defects, govern mass transport in crystalline solids, and are therefore fundamental to a wide variety of kinetic processes in materials. In pure metals, classic experiments on the thermodynamics of vacancies, self-diffusion, and the recovery of radiation damage provide a sound foundation of understanding. In semiconductors, however, even the most basic defect properties such as the formation and migration enthalpies of interstitials and vacancies remain controversial mostly because of the great difficulty of designing conclusive experiments [1–3]. For example, low temperature electrical conductivity and field ion microscopy [4] have provided detailed measurements of point-defect mobilities in metals, but these methods cannot be easily applied to Si, Ge, or III-V compound semiconductors.

Much of the current knowledge of point-defect motion in silicon is derived from spectroscopic methods: e.g., electron paramagnetic resonance [5], capacitance spectroscopy [6], and infrared absorption [7]. Recent diffuse x-ray scattering experiments on low temperature electron-irradiated [8] and ion-implanted silicon [9] suggest that conclusions drawn from these spectroscopic methods may be misleading because the spectroscopic probes are sensitive to only a small minority of the defects produced in a radiation damage experiment [10]. The added complexity of charge-state dependence of the defect structures and transition states, and strong interactions between point defects and impurity atoms have also hampered the interpretations of experiments [1].

We have approached the problem of point-defect motion in Si by using scanning tunneling microscopy (STM) to quantify surface defects created by He ion bombardment. Surface defects are created directly by the ion bombardment but bulk point defects that can diffuse to the surface, and which are of primary interest here, also contribute to the surface morphology [11]. We use the temperature dependence of the areal density of adatoms and adatom clusters, combined with supporting data from molecular dynamics simulations to isolate the contributions of bulk defect migration to the observed surface damage.

Our approach is closely related to the well-established method of field-ion microscopy (FIM) of radiation damage [4] and the more recent development of reflection high energy electron diffraction (RHEED) as a probe of surface disorder [11,12]. The equivalence of STM and FIM measurements of irradiated materials was recently demonstrated for ion-implanted Pt: an STM study [13] of interstitial motion following keV ion bombardment of Pt(111) closely replicated FIM data that were published nearly 30 years ago [14]. In RHEED studies, surface defects are detected by the decrease in the intensity of the half order $(0, 0, 1/2)$, i.e., "out-of-phase" specularly reflected electrons [11,12].

We clean Sb-doped Si(001) wafers by several cycles of rapid heating to 1300 °C in ultrahigh vacuum. The samples are transferred to the variable-temperature STM and imaged at room temperature to verify the quality of the surface. In this STM design, only the temperature of the sample is controlled; the temperature of the PtIr probe tip and surroundings remain near room temperature. Next, we cool the samples to 80, 130, or 180 K and bombard the sample with 4.5 keV He ions from a hot-filament ion source. Ions strike the surface at an angle of 60° from normal with the probe tip withdrawn by ~ 3 mm. The surface is then imaged at the same temperature. Secondary-ion mass spectroscopy (SIMS) measurements of the samples after removal from the STM chamber show that the dominant metallic impurities in the near-surface region are Sb (dopant), and Mo, Cu (contamination by the sample holder) with concentrations $\sim 10^{18}$ cm^{-3}.

Temperatures of the Si samples are measured indirectly by a diode thermometer mounted adjacent to the sample

 0031-9007/99/83(23)/4788(4)$15.00 © 1999 The American Physical Society

holder; the temperature difference between the sample and the thermometer was calibrated using a thermocouple attached to a test wafer. In the worst case, at $T = 80$ K, this temperature difference is ≈ 25 K.

The He ion flux is 5.7×10^{10} ions cm sec^{-1} at the sample; the He gas pressure in the STM chamber is $\approx 2 \times 10^{-8}$ Torr, and the background pressures of CO and H_2O are $\approx 1 \times 10^{-10}$ Torr. Ion flux is calibrated by measuring the total current collected by a test sample constructed from a Au-coated substrate. By biasing the gold film to < -10 V, secondary electrons are repelled from the surface and the measured current is the sum of the incident ion current and the current of secondary electrons. The secondary electron yield for He bombardment of Au in our geometry is ≈ 1.1 [15]. Samples are irradiated for 5 min (ion fluence of 1.7×10^{13} ions cm^{-2}), imaged by STM, irradiated for a second period of 5 min, and imaged again. These ion doses are intermediate to the range of ion doses investigated by Bedrossian [12].

Classical molecular dynamics (MD) simulations are used to provide a description of the defect state prior to defect migration. The temperature of the simulation box was set to 0 K at the beginning of each simulation. We simulated 1450 events with Si-Si interactions modeled by a modified form of the Tersoff semiempirical potential [16] and a purely repulsive potential for the He-Si interaction [17]. The simulation cell holds ≈ 2000 atoms; the Si(001) surface is given the 2×1 dimer reconstruction prior to starting the simulation. Periodic boundaries are used in the x-y directions with temperature scaling applied to these boundaries and to the bottom z surface. He atoms that reach a boundary are stopped. The system is evolved for 2 ps; after this length of time the structure of the simulation remains approximately constant. Vacancies and interstitials are identified by the number of atoms within each primitive cell of the lattice [16].

Figure 1 shows STM images of surface defects following ion bombardment. The density of surface vacancylike defects is mostly due to the large background density of "missing dimers defects" of the thermally cleaned surfaces prior to ion bombardment. Adatomlike defects (adatoms, ad-dimers and larger adatom clusters) are rarely observed on the initial surface, and therefore, we focus our analysis and discussion on our measurements of adatoms and adatom clusters. Also, since we cannot easily distinguish the number of adatoms in a surface protrusion, we will analyze all surface protrusions collectively and refer to them using the term "bright spot"—following the practice used for FIM [14].

We analyze each image by measuring the height h of each bright spot for bright spots with $h > 0.3a$, where a is the monolayer step height, $a = 0.136$ nm. An STM does not directly measure the heights of atoms—in general, STM topographies are determined by the small electronic state density at a distance of ~ 0.4 nm from the surface. Nevertheless, we have found that the measured heights of the bright spots with $h > 0.3a$ are reproducible and, at least for our imaging conditions of large negative sample bias (-2.7 V), relatively insensitive to the geometry and electronic structure of the probe tip. Measurements of bright spots with $h < 0.3a$ become increasingly unreliable with decreasing h, and for this reason we exclude those features from our analysis.

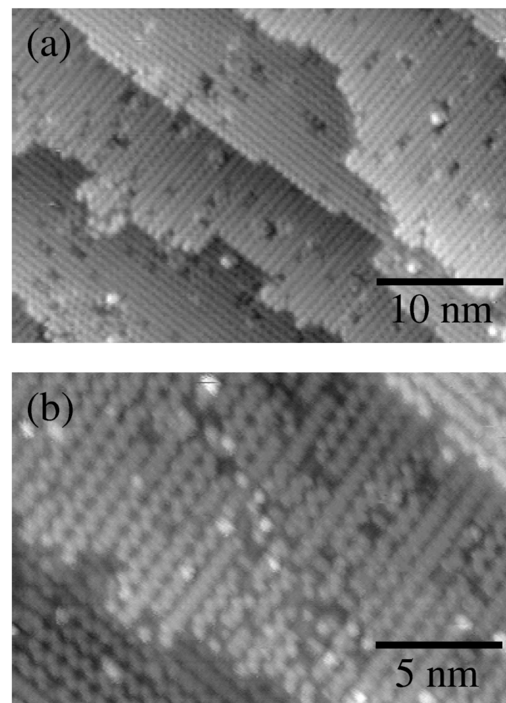

FIG. 1. STM images of Si(001) bombarded by 4.5 keV He ions at 180 K. (a) 1.7×10^{13} ions cm^{-2} and (b) 3.4×10^{13} ions cm^{-2}. The areas of the images are (a) 40×27 nm^2 and (b) 20×13 nm^2. Adatoms, dimers, and adatom clusters are visible as "bright spots" that are ~ 1 nm in diameter.

The analysis of ≈ 3000 bright spots is summarized in Fig. 2 where we plot histograms of heights for the 8 experimental conditions (4 temperatures, and 2 ion doses) we studied. All of the histograms have a peak near $h = a$. We tentatively identify the majority of bright spots with $h \approx a$ as ad-dimers since most are located at the center of dimer rows and are approximately circular, see Fig. 1. Ad-dimers can be created directly by the ion bombardment—approximately 40% of adatoms produced in the MD simulations are part of an ad-dimer or larger adatom cluster—but low temperature surface diffusion [18,19] must also play a role in their formation, particularly at $T > 180$ K.

In most cases, the histograms increase again at $h < 0.6a$ and appear to peak at $h < 0.3a$. The density of $h < 0.6a$ bright spots is particularly pronounced at 180 K and ion dose 3.4×10^{13} ions cm^{-2}. These $h < 0.6a$ bright spots are more widely distributed within the 2×1 surface reconstruction. We have chosen to focus our experiments

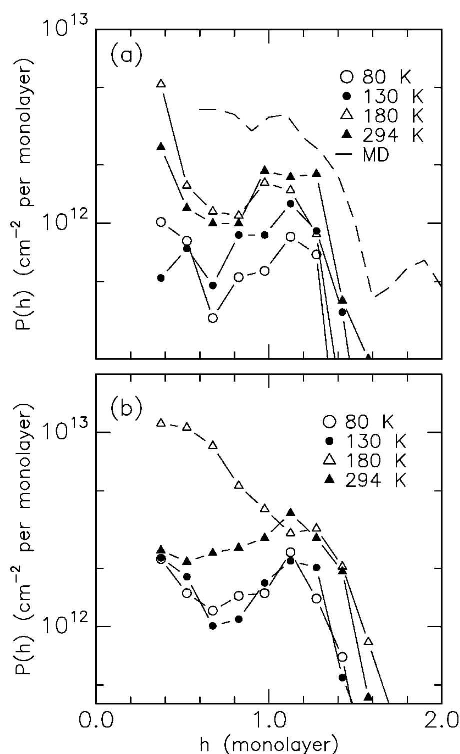

FIG. 2. Histograms of the heights of bright spots measured from STM images for ion doses of (a) 1.7×10^{13} ions cm^{-2} and (b) 3.4×10^{13} ions cm^{-2}. The data symbols are labeled by the temperature of the sample during ion bombardment and imaging. The height of one monolayer is $a = 0.136$ nm. The dashed line in (a) shows the calculated distribution of adatom heights from molecular dynamics simulations scaled to the same ion dose as the experiments.

on measurements of a large number of bright spots at moderate resolutions rather than a detailed analysis of a small number of bright spots at high resolution, but we note that a significant fraction appear similar to the off-center structures identified by Wolkow [18] as Si adatoms. Not all of these bright spots, however, can be confidently identified as isolated Si adatoms. Figure 2 shows that $h < 0.6a$ bright spots are also present on the 294 K surface. Since Si adatoms have not been observed during deposition at room temperature [20], we conclude that most of these structures are more complex than a simple adatom.

Figure 2a also includes a histogram of the heights of adatoms that are produced by our MD simulations. The similarity of the computational height distribution of adatoms to the experimental data is surprisingly good considering the limitations of this comparison: (i) the STM sees only adatom clusters, not individual adatoms and the STM heights are influenced by the electronic structure; and (ii) the MD results are dependent, of course, on the accuracy of the potentials and exclude activated processes because of the short simulation time (2 ps). The yield of adatoms produced in the MD simulations is a factor of ~ 3 larger than the measured density of bright spots at the lowest temperatures, 80 and 130 K.

To more clearly show the temperature dependence of the STM data, we plot in Fig. 3 the total areal density of bright spots with heights in the range $0.3 < h/a < 1.6$. The density is approximately constant at 80 and 130 K, is largest at 180 K, and has an intermediate value at 294 K. The lower density of bright spots at 294 K is probably caused by the healing of surface defects and surface diffusion of adatoms. We envision 3 atomic-scale processes that could become activated at $130 < T < 180$ K and produce the enhancement in the density of bright spots at 180 K: (i) migration of bulk vacancies to the surface and the subsequent creation of dimer vacancies [21] and adatoms; (ii) changes in the structure of surface defects that increase the fraction of adatomlike surface defects that are visible to the STM; and (iii) migration of bulk interstitials to the surface.

We can safely exclude the first mechanism since each additional bright spot would have to have to be associated with at least one missing dimer and the density of missing-dimer defects in the STM images does not increase significantly at 180 K. The activation of a surface mechanism is harder to rule out; in fact, an abrupt *increase* in RHEED specular intensity of ion irradiated Si(001) surface annealed at ≈ 160 K was interpreted as evidence of the annihilation of surface vacancies and adatoms [12]. Our data, however, would require a more complex mechanism that converts adatoms not detected by STM into bright spots.

We propose that the migration of bulk interstitials is the most satisfactory explanation of the enhanced density of bright spots at 180 K. This assertion is supported by diffuse x-ray scattering measurements of electron-irradiated Si [8] and Si bombarded by 4.5 keV He atoms

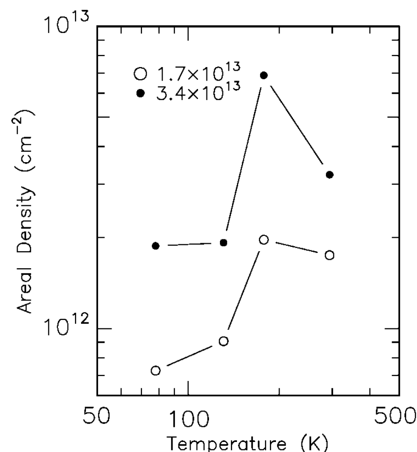

FIG. 3. Areal density of bright spots with heights in the range $0.3 < h/a < 1.6$ plotted as a function of temperature for both ion doses.

[9] that reveal the formation of interstitial clusters in this temperature range. To make a rough estimate of the migration energy E_m of the interstitials, we assume that the interstitial hopping rate is $\ll 1$ sec^{-1} at 130 K, and $\gg 1$ sec^{-1} at 180 K; and that the attempt frequency is given by the Debye frequency for Si, 14 THz; then $E_m \approx 0.4$ eV.

Finally, we discuss the range of interstitial migration that is consistent with our data. Figure 4 shows the depth distribution of defects calculated by MD simulation. To match our observed factor of ~ 3 increase in the bright-spot density at 180 K, we estimate that interstials in at least layers 1–13, i.e., interstitials within ~ 2 nm of the surface, would have to be trapped by the surface.

Carbon or other impurities may act as traps for interstitials [22] and limit the number reaching the surface from greater depths. Since we do not have a good measurement of the impurity concentration in the near-surface region—for example, SIMS measurements of near-surface C concentrations are strongly affected by adsorbed hydrocarbons—we are unable to provide a quantitative calculation of the migration distance. But we can make an order-of-magnitude estimate by assuming that interstials visit n/c atomic sites before becoming trapped by an impurity atom, where c is the trap density and n is the atomic density. An interstitial will therefore diffuse (by a random walk of n/c hops in three-dimensions) an average distance $l = (n/c)^{1/2}n^{-1/3}$ from its starting point; and $l/\sqrt{3}$ provides an estimate of the distance an interstitial will diffuse in one dimension; i.e. interstitials within $l/\sqrt{3}$ of the surface will reached the surface before being trapped by an impurity atom. For $n/c = 1000$, $l \approx 5$ nm, and within a factor of ~ 3 of what is needed to explain the enhanced density of bright spots at 180 K. In this discussion, we have assumed that the surface is a perfect sink for interstitials; the efficiency of surface trapping is, however, controversial and a topic of great current interest for understanding shallow doping of semiconductors using low-energy ion implantation [23–25].

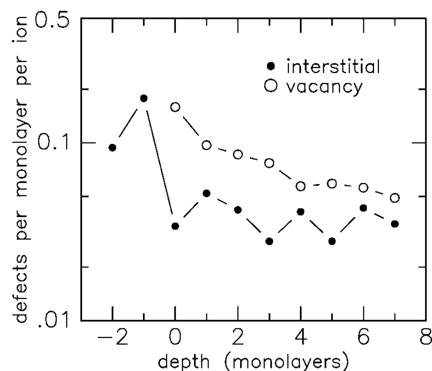

FIG. 4. Number of vacancies and interstitials as a function of depth calculated by classical molecular dynamics. Adatoms are plotted as layer number −1 and sputtered atoms are plotted as layer number −2.

This work was supported by National Science Foundation Grant No. DMR 96-32252, U.S. Department of Energy Grant No. DEFG02-96-ER45439, and the Academy of Finland under Projects No. 35073 and No. 44215; STM and SIMS measurements used the facilities of the Center for Microanalysis of Materials, University of Illinois, which is supported by the U.S. Department of Energy. We thank Vania Petrova for her expert assistance with the operation of the STM.

[1] P.M. Fahey, P.B. Griffin, and J.D. Plummer, Rev. Mod. Phys. **61**, 289 (1989).
[2] A. Seeger, Radiat. Eff. **9**, 15 (1971).
[3] T.Y. Tan and U. Gösele, Appl. Phys. A **37**, 1 (1985).
[4] David N. Seidman, Surf. Sci. **70**, 532 (1978).
[5] G.D. Watkins, J.R. Troxell, and A.P. Chatterjee, in *Defects and Radiation Effects in Semiconductors,* edited by J.H. Albany, IOP Conf. Proc. No. 46 (Institute of Physics and Physical Society, London, 1979), p. 16.
[6] J.C. Brabant *et al.,* J. Appl. Phys. **47**, 4809 (1976).
[7] B. Massarani and A. Brelot, in *Radiation Damage and Defects in Semiconductors,* IOP Conf. Proc. No. 16 (Institute of Physics and Physical Society, London, 1973), p. 269.
[8] P. Ehrhart and H. Zillgen, in *Defects and Diffusion in Silicon Processing,* edited by T. Diaz de la Rubia, S. Coffa, P.A. Stolk, and C.S. Rafferty, MRS Symposia Proceedings No. 469 (Materials Research Society, Pittsburgh, 1997), vol. 469, p. 175.
[9] K. Nordlund *et al.,* Nucl. Instrum. Methods Phys. Res., Sect. B **147**, 399 (1999).
[10] P. Ehrhart and H. Zillgen, J. Appl. Phys. **85**, 3503 (1999).
[11] J.A. Floro *et al.,* J. Appl. Phys. **77**, 2351 (1995).
[12] Peter J. Bedrossian and Tomas Diaz de la Rubia, J. Vac. Sci. Technol. **16**, 1043 (1998).
[13] Markus Morgenstern, Thomas Michely, and George Comsa, Phys. Rev. Lett. **79**, 1305 (1997).
[14] P. Pétroff and D.N. Seidman, Appl. Phys. Lett. **18**, 518 (1971).
[15] H. Eder *et al.,* Rev. Sci. Instrum. **68**, 165 (1997).
[16] J. Tarus *et al.,* Phys. Rev. B **58**, 9907 (1998).
[17] K. Nordlund, N. Runeberg, and D. Sundholm, Nucl. Instrum. Methods Phys. Res., Sect. B **132**, 45 (1997).
[18] Robert A. Wolkow, Phys. Rev. Lett. **74**, 4448 (1995).
[19] A.P. Smith and H. Jónsson, Phys. Rev. Lett. **77**, 1326 (1996).
[20] Peter J. Bedrossian, Phys. Rev. Lett. **74**, 3648 (1995).
[21] Zhenyu Zhang and H. Metiu, Phys. Rev. B **48**, 8166 (1993).
[22] M.D. Johnson, M.-J. Caturla, and T. Diaz de la Rubia, J. Appl. Phys. **84**, 1963 (1998).
[23] D.R. Lim, C.S. Rafferty, and F.P. Klemens, Appl. Phys. Lett. **67**, 2302 (1995).
[24] Aditya Agarwal *et al.,* Appl. Phys. Lett. **70**, 3332 (1997).
[25] H.-J. Gossmann *et al.,* Appl. Phys. Lett. **67**, 1558 (1995).